

# Three-dimensional ultrastructure and histomorphology of mouse circumvallate papillary taste buds before and after birth using focused ion beam-scanning electron microscope tomography

Kiyosato Hino<sup>a,b,\*</sup>, Shingo Hirashima<sup>a,b</sup>, Risa Tsuneyoshi<sup>a</sup>, Akinobu Togo<sup>c</sup>, Tasuku Hiroshige<sup>d</sup>, Jingo Kusukawa<sup>b</sup>, Kei-Ichiro Nakamura<sup>a,e</sup>, Keisuke Ohta<sup>a,c</sup>

<sup>a</sup> Division of Microscopic and Developmental Anatomy, Department of Anatomy, Kurume University School of Medicine, Kurume 830-0011, Japan

<sup>b</sup> Dental and Oral Medical Center, Kurume University School of Medicine, Kurume 830-0011, Japan

<sup>c</sup> Advanced Imaging Research Center, Kurume University School of Medicine, Kurume 830-0011, Japan

<sup>d</sup> Department of Urology, Kurume University School of Medicine, Kurume 830-0011, Japan

<sup>e</sup> Cognitive and Molecular Research Institute of Brain Diseases, Kurume University School of Medicine, Kurume 830-0011, Japan

## ARTICLE INFO

### Keywords:

Taste buds  
Development  
Mice  
FIB-SEM  
Three-dimensional reconstruction

## ABSTRACT

Early taste buds are formed from placode cells. Placode cells differentiate into Type I–III cells at birth; however, the ultrastructure of these first taste cells remain elusive. Here, we used focused ion beam-scanning electron microscopy (FIB-SEM) to analyze taste buds on the dorsal surface of the circumvallate papilla on embryonic day (E) 18.5 and postnatal day (P) 1.5. The taste buds on E18.5 existed as a mass of immature cells. One of the immature cells extended the cell process to the surface of the epithelium from the taste bud mass. Cytoplasm of this cell contained many mitochondria and vesicles in the apical region. The taste buds at P1.5 had small taste pores and had an onion-shaped structure. Most of the cells in the taste buds extended toward the taste pores. Some of the cells in the taste buds were Type II-like cells with glycogen in their cytoplasm. In this study, it was shown in three dimensions that immature cells extend to the surface of epithelium before the formation of the taste pore. Subsequently, the formation of taste pores and maturation of taste buds progress simultaneously.

## 1. Introduction

Taste buds are organs located on the lingual papillae and soft palate and are responsible for gustation. Each taste bud contains approximately 25–80 taste cells (Ogata and Ohtubo, 2020). Taste cells were classified as Type I (dark), Type II (light), Type III (intermediate), and Type IV based on their ultrastructural features using transmission electron microscopy (TEM) (Kinnamon and Yang, 2008) (Supplementary data). Type I cells are glial-like cells and express a variety of transporters and ion channels. Type II cells are receptor cells that detect sweet, bitter, or umami tastes. Type III cells include sour taste receptive cells (Chaudhari and Roper, 2010; Kinnamon and Yang, 2008; Liman et al., 2014). Type IV cells lie at the basolateral margin of the taste bud and represent the

immature cells that eventually differentiate to Type I–III cells (Miura et al., 2014; Yang et al., 2020).

The mouse taste placodes appear as foci of columnar epithelium concentrated in area that becomes the fungiform papillae (FFP) and circumvallate papillae (CVP) by embryonic day (E)12.5 (Mistretta and Liu, 2006). The trenches of CVP begin to form by E13.5, and papillae with a mesenchymal core are created by E14.5 (Kim et al., 2009; Nakayama et al., 2008). Gustatory nerve fibers reach and penetrate the apical papillary epithelium during E13.5–15.5 (Hall et al., 1999; Kapsimali and Barlow, 2013; Krimm et al., 2015). Although onion-shaped cellular concentrations in the papillary epithelium finally differentiate into taste buds, they are generally considered mature when taste pores form in the first postnatal week (Zhang et al., 2008). At birth, the entire

**Abbreviations:** 3D, three-dimensional; CVP, circumvallate papillae; E, embryonic day; FFP, fungiform papillae; FIB-SEM, focused ion beam-scanning electron microscopy; P, postnatal day; PFA, paraformaldehyde; PBS, phosphate-buffered saline; SEM, scanning electron microscopy; TEM, transmission electron microscopy; SBF-SEM, serial block-face scanning electron microscopy.

\* Corresponding author at: Division of Microscopic and Developmental Anatomy, Department of Anatomy, Kurume University School of Medicine, 67 Asahi-machi, Kurume-shi, Fukuoka 830-0011, Japan.

E-mail address: [kiyosato\\_hino@med.kurume-u.ac.jp](mailto:kiyosato_hino@med.kurume-u.ac.jp) (K. Hino).

<https://doi.org/10.1016/j.tice.2021.101714>

Received 9 September 2021; Received in revised form 13 December 2021; Accepted 14 December 2021

Available online 22 December 2021

0040-8166/© 2022 The Authors. Published by Elsevier Ltd. This is an open access article under the CC BY license (<http://creativecommons.org/licenses/by/4.0/>).

taste bud is composed of 7–13 cells that express Shh and K8 (Kramer et al., 2019; Thirumangalathu et al., 2009). These cells are the precursor cells of taste cells and differentiate directly into Type I, II or III cells and gradually disappear after birth (Golden et al., 2021). Zhang and colleagues reported that in the mouse CVP, no matured taste buds with taste pores are found at birth; however, the taste pores gradually form after birth (Zhang et al., 2008). Instead, taste buds fully differentiate in the postnatal week (Barlow, 2015; Kapsimali and Barlow, 2013). Nevertheless, immunohistological studies have shown that taste cells are differentiated before birth (Golden et al., 2021; Thirumangalathu and Barlow, 2015). It is not known whether embryonic cells or postnatal cells are involved in the formation of taste pores, which is considered a sign of maturation. Moreover, there is little evidence of the detailed morphology of these immature taste precursor cells that appear before birth (Farbman, 1965). Therefore, we here attempted to perform further morphological studies to understand this long standing question.

Electron microscopy is useful for analyzing the detailed structure of taste buds. Particularly, three-dimensional (3D) observations have been useful for understanding the detailed cellular architecture of taste buds (taste cells) and their cellular composition. In the early 90 s, the 3D reconstruction analysis of taste cells was performed using serial sections obtained by TEM (Royer and Kinnamon, 1994, 1991; Seta and Toyoshima, 1995). However, 3D reconstructions using TEM images have several disadvantages, such as limited imaging range, huge time consumption, and technical difficulty (Denk and Horstmann, 2004).

Recently, volume imaging using scanning electron microscopy (SEM) has been developed that enables analysis of the 3D ultrastructure of tissue organization. Several volume SEM techniques have been developed, including serial block-face SEM (SBF-SEM), array tomography, and focused ion beam-SEM (FIB-SEM) tomography, and all of them are based on serial image acquisition (Denk and Horstmann, 2004; Knott et al., 2008; Kremer et al., 2015; Micheva and Smith, 2007; Ohta et al., 2012). Matured taste buds have also been analyzed using SBF-SEM to observe the cytoplasmic features, 3D structures, and distribution of taste cells in taste buds (Yang et al., 2020). Therefore, volume imaging methods using SEM show great promise for the analysis of the taste buds comprising multiple cells. Among the several volume SEM imaging methods described above, FIB-SEM tomography can reconstruct 3D structures from a wide range of high-resolution images of the material surface and with a high depth resolution (Kato et al., 2007). Since immature taste buds in the CVP are scattered in the papillary epithelium and their distribution is not uniform, capturing the image of the whole taste bud is difficult and can only be achieved by chance. Therefore, FIB-SEM tomography, which can acquire the image of the target portion from a large area, is suitable for observing immature taste buds.

In this study, we selected two developmental stages of taste buds to analyze the 3D ultrastructure of immature taste buds: E18.5, just before birth, and P1.5, at the beginning of the development of taste stimulation. We investigated the features of the overall structure of the immature taste buds and the different taste bud cell types that constitutes the taste buds.

## 2. Materials and methods

### 2.1. Animals

One wild-type male and two C57BL/6J female mice were used in this study. All mice were bred at the animal facility of our institution. They were housed under a constant 12 h light/dark cycle (lights on at 7:00 am), fed a standard laboratory diet, and allowed free access to food and water. Male and female mice were allowed to live together overnight. Mating was assumed to occur between 6:00 pm and midnight, and E0.5 was defined as the day on which the plug was confirmed the next morning. On E18.5, one pregnant mouse was anesthetized with a combination of anesthetics (0.3 mg/kg medetomidine, 4.0 mg/kg midazolam, and 5.0 mg/kg butorphanol), and six fetuses were removed

from the uterus and used for further analyses. The gestation length of the second mice was 19 days. Six P1.5 neonates were sacrificed by decapitation and used for further analyses. A scheme of the experimental procedures is described in Fig. 1.

All experiments were performed in accordance with the National Institutes of Health guidelines for animal research. All animal experiments were approved by the Institutional Animal Care Committee of Kurume University, Fukuoka, Japan.

### 2.2. Hematoxylin and eosin (H&E) staining

The tongues were removed from the E18.5 fetuses and P1.5 neonates (n = 2, each). Dissected tongues were immersed in 4% paraformaldehyde (PFA) in phosphate-buffered saline (PBS) for 2 h at 4 °C. The specimens were subsequently trimmed (2 × 3 mm size), washed three times for 5 min in PBS, and processed to prepare 5 μm-thick paraffin sections. The sections were stained with hematoxylin and eosin (H&E) and subsequently imaged with a fluorescence microscope (BZ-X710, KEYENCE).

### 2.3. Tissue preparation for SEM

The tongues were removed from the E18.5 fetuses and P1.5 neonates (n = 4, each). The specimens were immersed in a half-Karnovsky solution (2% paraformaldehyde, 2.5% glutaraldehyde, 2 mM CaCl<sub>2</sub> in a 0.1 M cacodylate buffer) for 2 h at 4 °C, washed in 0.1 M cacodylate buffer, and then trimmed to 1 mm × 2 mm sizes. After three washes with cacodylate buffer, the specimens were post-fixed for 1 h in a solution containing 2% osmium tetroxide in cacodylate buffer at 4 °C, washed three times with distilled water (DW), and immersed in 1% thiocarbonylhydrazide solution for 1 h. After three washes with DW, the specimens were further immersed in 2% osmium tetroxide in DW and washed three times with DW. Thereafter, they were dehydrated in an ethanol series (25%, 50%, 70%, 80%, 90%, and twice in 100% ethanol for 5 min each). Subsequently, the samples were freeze-dried with tert-butyl alcohol, mounted on a metal stub, sputter-coated with carbon, and examined using SEM (Quanta 3D FEG; FEI, Eindhoven, The Netherlands).

### 2.4. Sample preparation, volume image acquisition, and 3D ultrastructural analysis by FIB-SEM tomography

Tissue preparation, FIB-SEM tomography, and 3D ultrastructural analysis were performed following the procedures described in our previous studies (Hirashima et al., 2016; Ohta et al., 2012).

#### 2.4.1. Tissue preparation for FIB-SEM tomography and en bloc staining

The specimens were immersed in the same fixative used for tissue preparation of SEM for 2 h at 4 °C, rinsed in the same buffer (Section 2.3), and fixed with 1.5% potassium ferrocyanide and 2% osmium tetroxide for 1 h at 4 °C. After rinsing with DW, the specimens were treated with 1% thiocarbonylhydrazide, rinsed with DW, immersed in a 2% osmium tetroxide solution for 1 h at 37 °C, and washed again with DW. For en bloc staining, the specimens were immersed in a 4% uranyl acetate solution overnight and washed with DW. The specimens were stained with Walton's lead aspartate solution. They were dehydrated in an ice-chilled ethyl alcohol gradient series and acetone, then embedded in epoxy resin (Epon812; TAAB Laboratories Equipment Ltd., Berkshire, UK), and polymerized for 48 h at 65 °C.

#### 2.4.2. FIB-SEM tomography

The resin blocks were placed on a metal stub. The surfaces of the embedded specimens were exposed using a diamond knife on an Ultracut E microtome (Leica, Wetzlar, Germany). The metal stub with the specimens was set on the stage of FIB-SEM (Quanta 3D FEG; FEI, Eindhoven, The Netherlands). Serial images of the block face were

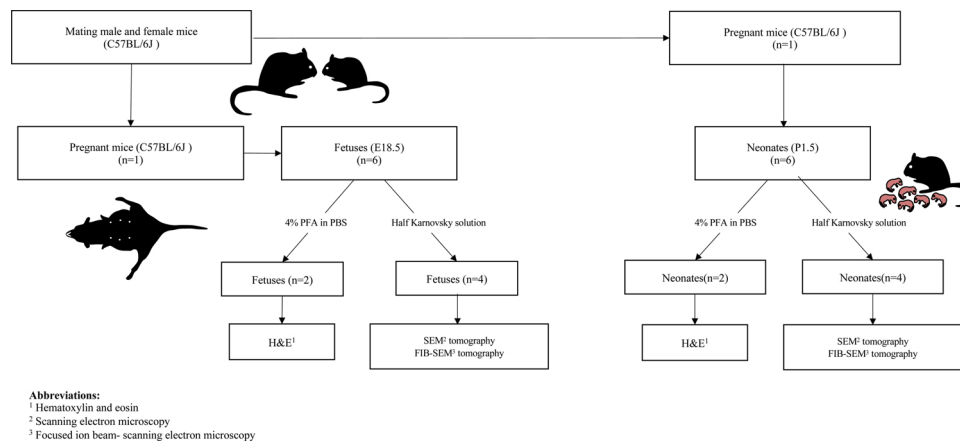


**Fig. 1.** Flow diagram of the study design. Flow diagram showing the selection strategy of animals for the experiment. In this study, we used the fetuses of Embryonic day (E) 18.5 and neonates of postnatal day (P) 1.5. The immature taste buds collected from E18.5 fetuses and P1.5 neonates were classified using conventional methods (Kinnaman and Yang, 2008).

acquired by repeated cycles of sample surface milling and imaging using the Auto Slice & View G2 operating software (FEI). Milling was performed with a gallium ion beam at 30 kV with a current of 15 nA. The milling pitch was set to 50 nm/step and 750–800 cycles. Images were acquired at landing energy of 5.0 keV. Additional acquisition parameters were as follows: beam current = 0.15 nA, dwell time = 6  $\mu$ s/pixel, image size = 2048  $\times$  1768 pixels, and pixel size = 29.1 nm/pixel. Serial images of the block face were acquired by repeated cycles of sample surface milling using a focused gallium ion beam and image acquisition using SEM. The resultant image stack was 30  $\times$  30  $\times$  75–80  $\mu$ m block size. 3D reconstruction was performed using the images obtained from the area containing the taste buds.

#### 2.4.3. 3D-structure reconstruction and image analysis

Serial section images were reconstructed into 3D images and analyzed using the 3D visualization software Avizo Ver.9.1.1 (FEI Visualization Science Group, Burlington, MA). In this FIB-SEM imaging, we mainly used the low-power field to include the entire taste bud from

the angle of view. In image analysis, the cells sharing a clear boundary with the surrounding epithelial cells and having low electron density were considered to be immature taste cells. We analyzed the morphology of these cells.

### 3. Results

#### 3.1. Analysis of taste cells at E18.5

##### 3.1.1. Light microscopy (LM)

At E18.5, hematoxylin and eosin staining results demonstrated that the CVP did not have a mature morphology, and the upper part was small and round. The surrounding trenches were not formed, and the epithelium was connected. These papillae were covered with a thin stratified squamous epithelium, and immature taste buds were located in the apical epithelium of the CVP. There were no obvious taste pores (Fig. 2A). Immature taste buds were approximately 20–30  $\mu$ m in diameter and had a clear boundary with the surrounding epithelium.

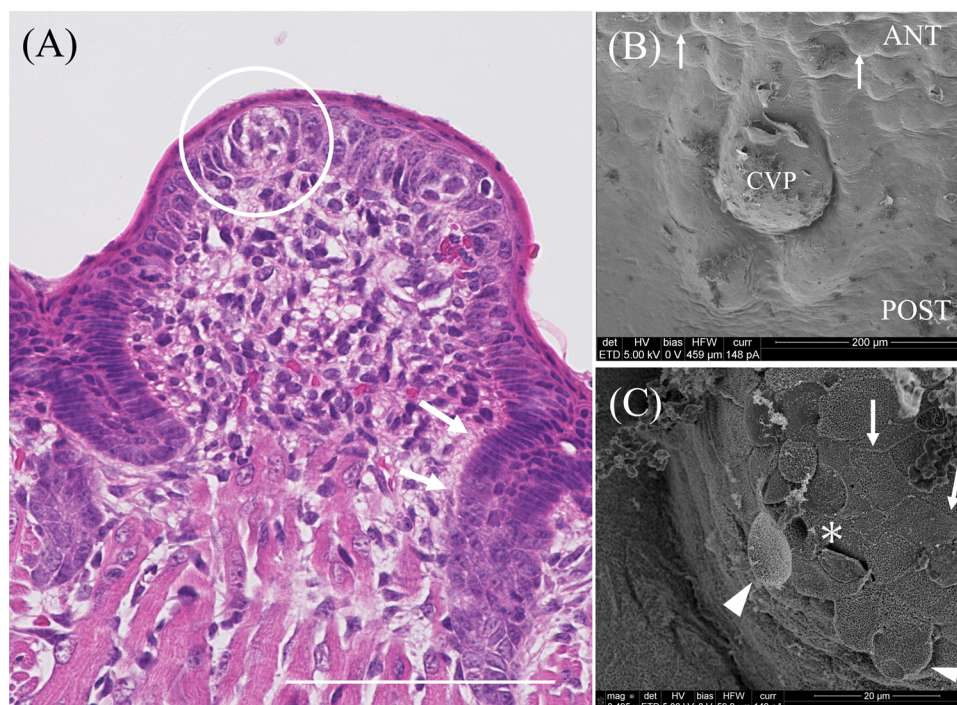


**Fig. 2.** Hematoxylin & eosin (H&E)-stained sections of the circumvallate papilla (CVP) at E18.5. **A.** The CVP does not have a typical mature morphology and still looks like a hill-ock. The trench is barely formed and has epithelial connections (arrow). Immature taste buds can be seen at the top of the epithelium of the CVP (white circle). The size of the immature taste bud is approximately 20  $\mu$ m. There are no taste buds in the epithelium of the trench surrounding the CVP. Scale bar: 100  $\mu$ m. **B.** Scanning electron microscopy images of the CVP at E18.5. The CVP is flat in front and circular in the rear. It is approximately 200  $\mu$ m in size, anterior (ANT) to posterior (POST), and 130  $\mu$ m laterally. The surrounding epithelium is smooth. The epithelium of the CVP is detached compared to the surrounding epithelium. The filiform papillae were small and round at the tip (arrow). **C.** Enlarged figure of the CVP surface. There are several detached epithelia (arrowheads). The black pores, which appear to be taste pores, are shadows caused by ablation (asterisks); arrow, cell border.

Intercellular junctions were loose, and intercellular bridges could be seen more clearly than in the surrounding epithelium.

### 3.1.2. SEM

In SEM, surface of the E18.5 CVP was flat at the tip and circular posteriorly. The surrounding trenches of the CVP were shallow. The filiform papillae were small and round at the tip (Fig. 2B). The surface epithelium was severely detached. Taste pores were not observed at the top surface of the papillae in the SEM images (Fig. 2C).

### 3.1.3. FIB-SEM tomography

**3.1.3.1. Appearance and cell types of taste bud.** In FIB-SEM images, almost all taste bud architecture was within the reconstructed volume (Fig. 3). The taste bud was located in the apical epithelium of the CVP. The taste bud at E18.5 was spherical and not in an onion-shaped cellular arrangement as seen for a typical mature taste bud. The 3D reconstruction showed that the immature cell (blue cell) had extended an apical process to the surface of epithelium from the mass of taste cells (Fig. 3A, arrow). There was no taste pore formation or direct access to the oral cavity at E18.5 even in 3D observation. In addition, there was no obvious microvilli formation. The bundle of nerve fibers penetrated the basement membrane from the connective tissue. These bundles were formed by many thin nerve fibers, which we considered as a whole (Fig. 3A). The bundle of nerve fibers became thin nerve fibers and ran in and around the taste buds. Although the nerve fibers were proximal to taste bud cells, synaptic vesicles could not be detected at the data resolution used in this study.

We classified the taste bud cells based on the electron density of the cytoplasm, the overall shape of the cell, and the shape of the nucleus and numbered using the same numbering systems (Fig. 3B). The immature cells (No. 1–9) had low electron density and some had cell depressions and nuclear membrane invaginations. In addition, most immature cells lacked a clear orientation, and were intertwined with each other (Fig. 3B, No. 1–8). Among these cells, one extended from the taste bud to the epithelial surface layer (Fig. 3B, No. 9). This cell had a lower electron density than other immature cells and a round nucleus with no nuclear membrane invagination. Basal cells (No. 10–13) that were in contact with the basement membrane had a higher electron density than immature cells and thin cytoplasm and oval nuclei (Fig. 3B).

**3.1.3.2. Immature taste cells.** Most immature cells did not have a unified

orientation. They also did not extend their processes to the surface layer of the epithelium (Fig. 4A, red). Instead, cells existed in complex intertwining with the surrounding cells. The electron density was in the middle of the E18.5 taste bud cells. The position of the nucleus also varied, with some located at the top of the taste bud and others at the bottom; however, no fixed pattern was observed (Fig. 4A). Moreover, the distribution of the nucleolus was even, and heterochromatin was attached to the nuclear membrane (Figs. 4A and 5 A, red cells). The shape of the nucleus varied from oval to triangular and showed invaginations of the nuclear membrane (Fig. 4A, No. 5, white arrowheads) or nerve fibers (Fig. 4B, No. 5, white arrowheads). 3D reconstructed images also confirmed that the nucleus was in close to nerve fibers (Fig. 4C and D). Some nuclei of immature cells (Fig. 4E, No. 2) had deep invaginations, similar to Type III cells. However, these invaginations were not continuous and did not extend to the opposite side, and never divide the nuclei into two in the 3D reconstructed image (Fig. 4F).

There was a cell that deviated from the mass of taste bud among the immature cells. This cell was characterized as extending to the surface of epithelium from the taste cell mass (Fig. 5A). This cell (Fig. 5A, No. 9) had a lower electron density than the other cells. The nucleus was mostly round and smooth. There were many chromatin molecules in the nuclei. Unlike the other cells, the cell body that extends from the taste bud exists just below the epithelial surface layer (Fig. 5B–E). At this stage, the cell body had not gained access to the oral cavity. Moreover, some low-electron-density vacuolar structures could be observed within the cell process (Fig. 5B, D, E) and aggregation of mitochondria were also observed around the structures (Fig. 5C, white arrows). 3D reconstruction revealed four low-electron-density structures in the process (Fig. 5F).

**3.1.3.3. Basal cell.** The basal cells within the taste bud were found in the basolateral region and in contact with the basement membrane (Fig. 6, dark purple). These cells had an electron-dense cytoplasm and were morphologically similar to the surrounding epithelial cells (Fig. 6). They (No. 10–13) had oval, irregular nuclei with scattered heterochromatin and relatively thin cytoplasm (Fig. 6). The bundle of nerve fibers ran from the connective tissue, crossed the basement membrane, and passed between the basal cells into the taste buds (Fig. 6A, D). Basal cells were flattened cells that lie along the basolateral margin of the taste bud (Fig. 6E).

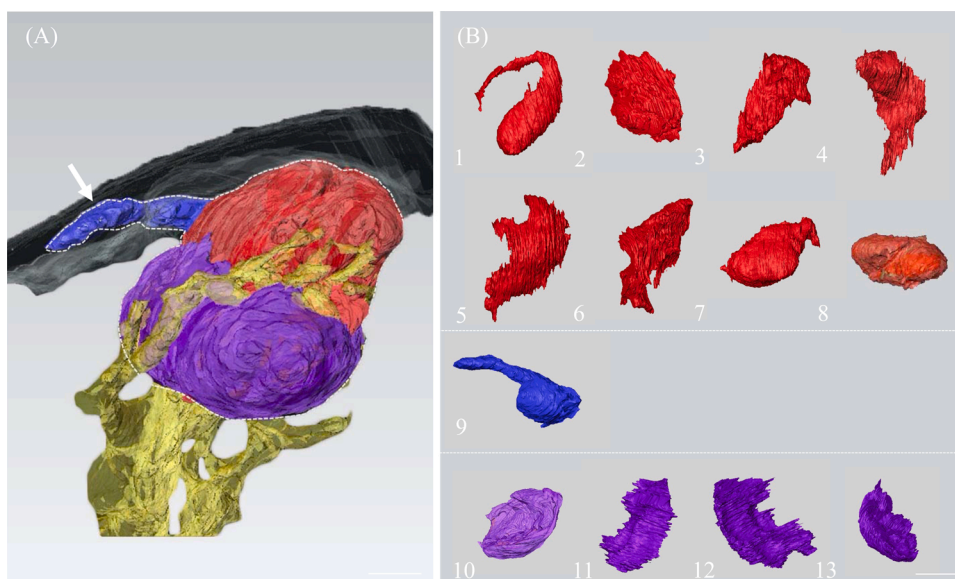


**Fig. 3.** 3D reconstructed image of the entire E18.5 CVP taste bud and each cell. **A.** The taste bud is not onion-shaped but is spherical instead (white dotted line). One of the immature cells extends an apical process to the epithelial surface layer (arrows). Nerve fibers enter and run from the connective tissue into the taste bud (yellow). Scale bar: 10  $\mu$ m. **B.** The red cells (No. 1–8) are classified as immature taste cells, each showing a different and diverse cell morphology. Some cells elongate up, down, left, and right (in three dimensions) without directionality. The immature taste cells exist as if they are pushing against each other, resulting in a distorted morphology. The immature cell (No. 9, blue) that deviate from the taste bud extends the cell process and has an orientation. The dark purple cells (No. 10–13) are flattened and bowl-shaped. Basal cells do not have a cell process. Scale bar: 10  $\mu$ m.

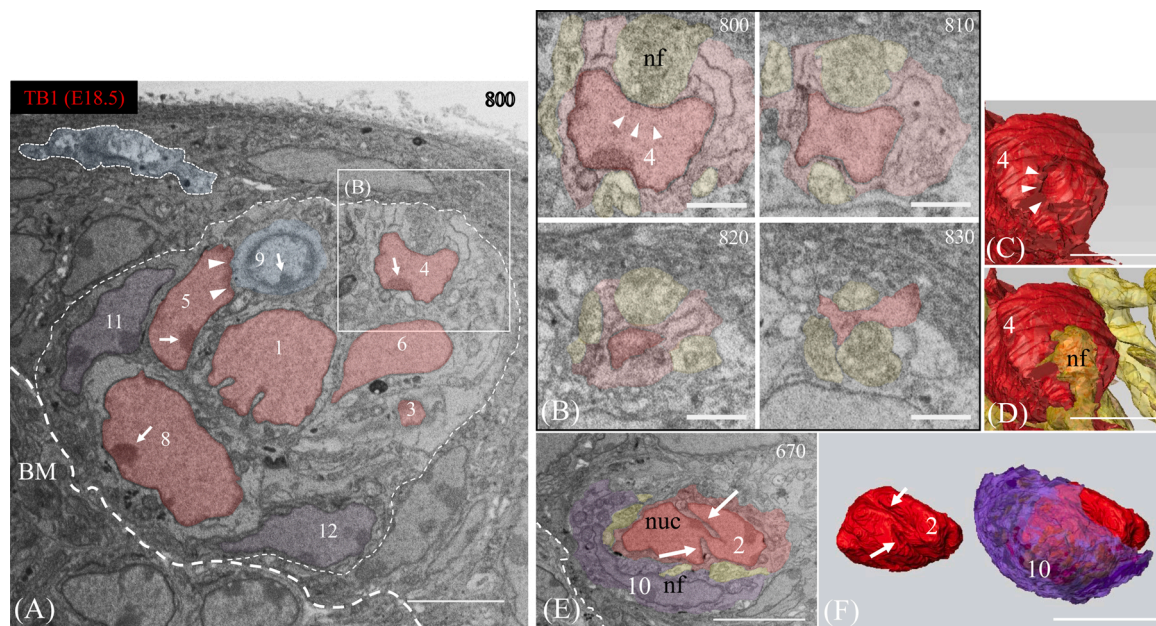


**Fig. 4.** Serial cross-sections of FIB-SEM tomography at E18.5. Various shapes of immature taste cells and their nuclei. **A.** Slice number 800 at E18.5. Immature taste cells have an intermediate electron density in taste cells and are painted red in this study. The immature taste cells elongate to fill gaps within a defined area. The nucleus of the immature cell has depressions because it is compressed by other cells and nerve fibers (arrowhead). Heterochromatin attached to the nuclear membrane (arrow). The immature cell (No. 8) is located at the center of the basal part of the taste bud and has an oval nucleus. Immature cell which extends to the surface of epithelium is blue, and basal cells are purple. The thin white dotted line represents the boundary of the taste bud. The thick white dotted line represents the basement membrane (BM). Scale bar: 10  $\mu\text{m}$ . **B.** Serial cross-sections of the focused ion beam-scanning electron microscope tomography (FIB-SEM). Magnified view of the square in **A** (slice no. 800). The nucleus of the cell (No. 4) features invagination of the membrane (arrowhead). The edge of the nuclei lies in close proximity with the nerve fibers and features invaginations of the membrane, which is evident in serial images (800–830). nf, nerve fibers; Scale bar: 3  $\mu\text{m}$ . **C, D.** Three-dimensional (3D) reconstructed images of the nucleus and nerve fibers in No. 4. Depressed nuclear area (arrowhead). **E.** Another section (slice number: 670). Some immature taste cells (No. 2) have deep nuclear invaginations. The white dotted line represents the basement membrane. nf, nerve fibers; Scale bar: 10  $\mu\text{m}$ . **F.** 3D reconstructed image of the nucleus of No. 2. The deep invagination of the nucleus is not connected (white arrow). There is a basal cell (No. 10) between this immature cell (No. 2) and the basement membrane. Scale bar: 5  $\mu\text{m}$ .

### 3.2. Analysis of taste cells at P1.5

#### 3.2.1. LM

At P1.5, hematoxylin and eosin staining revealed typical morphology of CVP, but the surrounding trenches were shallow. The epithelium in the trenches began to partially detach from each other. These papillae were covered with stratified squamous epithelium, and taste buds were found within the epithelium in apical and the trench area (Fig. 7A). Obvious taste pores could not be observed by conventional H&E-stained sections.

#### 3.2.2. SEM

In the SEM image, the CVP was pointed at the tip and circular at the posterior end (Fig. 7B). The epithelial detachment was less evident in the CVP on P1.5, and the trench surrounding the CVP was shallow. There were some pores in the epithelium. However, it was not clear whether these pores were taste pores (Fig. 7C). Typical diameter of the pore was approximately 1  $\mu\text{m}$  (Fig. 7C'). No microvilli structures were observed in the interior of the pores.

#### 3.2.3. FIB-SEM tomography

**3.2.3.1. Appearance and cell types of taste bud.** In the FIB-SEM volume analysis, we present an example of a single taste bud that includes almost the entire structure within the volume. The 3D reconstructed images showed that the taste bud of P1.5 was onion-shaped, similar to those of adult animals (Fig. 8A). The taste cells were directional and elongated toward the epithelial surface layer. Intriguingly, we found the formation of taste pore at this stage (Fig. 8B). Although the taste pore was still small, it could be clearly observed in the 3D reconstructed

images. A bundle of nerve fibers penetrated the basement membrane from the connective tissue and entered the taste bud. These bundles were formed by many thin nerve fibers, and we traced the nerve as a whole (Fig. 8A). The bundles of nerve fibers became thin nerve fibers and branched off from each other within the taste bud. Despite the proximity of nerve fibers with taste bud cells, synaptic vesicles could not be detected at this data resolution.

We classified the taste bud cells into four types based on their characteristics. These cells were numbered, and each number in Figs. 8–11 indicate the same cell in reconstructed volume (Fig. 8C). The type I-like cells had a slightly higher electron density, and the nucleus was oval and elongated. The nuclei of this cell had little invagination, and the cytoplasm was thin. Type II-like cells had low electron density and round nuclei with heterochromatin attached to the nuclear membrane (Fig. 8C, No. 9–11). Many dense granules were present in the cytoplasm. Type IV cells were located in the basal region and had higher electron density than the other cells. They had irregular nuclei and thin cytoplasm (Fig. 8C, No. 12–16). The pleomorphic cells showed a variety of morphologies, and the electron density was intermediate between Type I-like and Type II-like cells (Fig. 8C, No. 1–7). Some polymorphic cells had cytoplasmic depressions and deep invaginations in the nuclear membrane.

**3.2.3.2. Type I-like cell.** Cells that extended an apical process in the taste pore and had a slightly higher electron density in the cytoplasm were classified as Type I-like cells (Fig. 9A, No. 8). The nucleus of this cell was located at the middle of the taste buds and was oval and elongated. Patches of heterochromatin were observed in the nuclear membrane (Fig. 9A, No. 8). Many nerve fibers ran around this cell, and closely related areas were observed in the middle portion of this cell

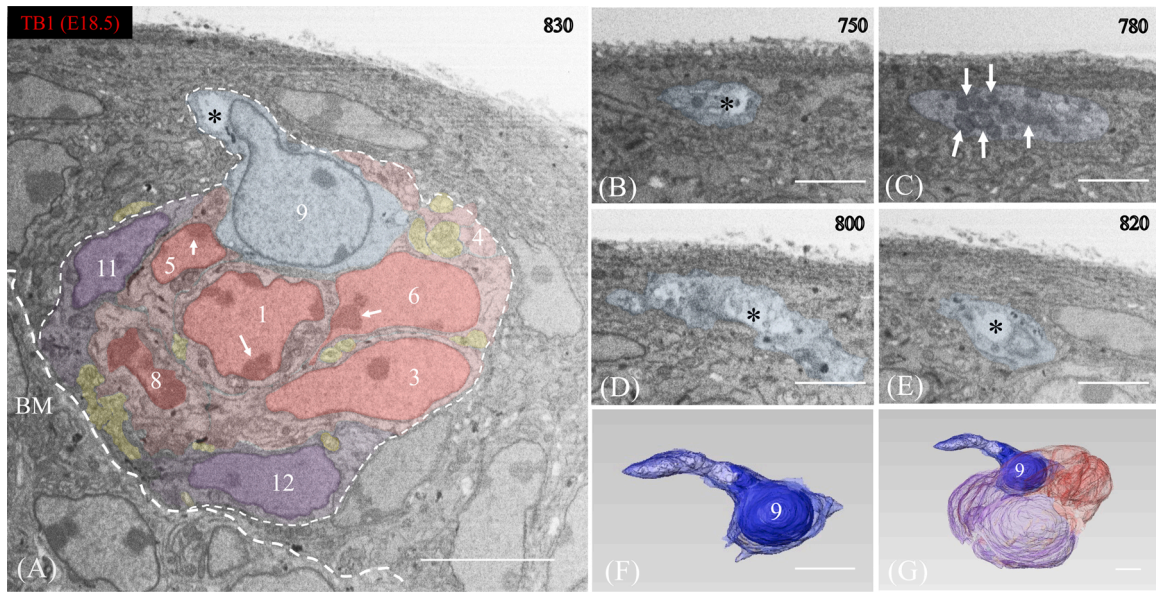


**Fig. 5.** Serial cross-sections of FIB-SEM tomography at E18.5. One of the immature cells that extend from the taste buds extends an apical process to reach just below the epithelial surface layer. **A.** Slice number 830. One of the immature cells extend from taste buds. This cell has a cytoplasm with a low electron density than the other immature cell. The nucleus of the cell is round, but the nucleus is partially projected in the extending cell body. There is a low electron density structure near the projected nucleus (asterisk). Heterochromatin of the immature cell is attached to the nuclear membrane (arrow). The thin white dotted line represents the boundary of the taste bud. The thick white dotted line represents the basement membrane (BM). Scale bar: 10  $\mu\text{m}$ . **B–E.** Slice numbers 750 to 820. In serial cross-sections, this cell (No. 9) extending from the taste bud is seen just below the epithelial surface layer, and taste pore is not formed. The extending cytoplasm contains several structures with apparently low electron densities (**B**, **D**, and **E**, asterisk). These structures are not single vesicle-like structures but are continuous. Some mitochondria are present at the tip of the cell (slice number 780, white arrow). Scale bar: 3  $\mu\text{m}$ . **F:** 3D reconstructed images of extending cell. Light blue indicates the cell body, and dark blue represents the nucleus. A part of the nucleus extends into the apical process of the cell. The four white structures are the low-electron-density structures observed in the serial cross-sections. Scale bar: 5  $\mu\text{m}$ . **G:** 3D reconstructed image of the whole taste bud as in (**A**), with the cell in No. 9 extending outward from the taste bud. Scale bar: 5  $\mu\text{m}$ .

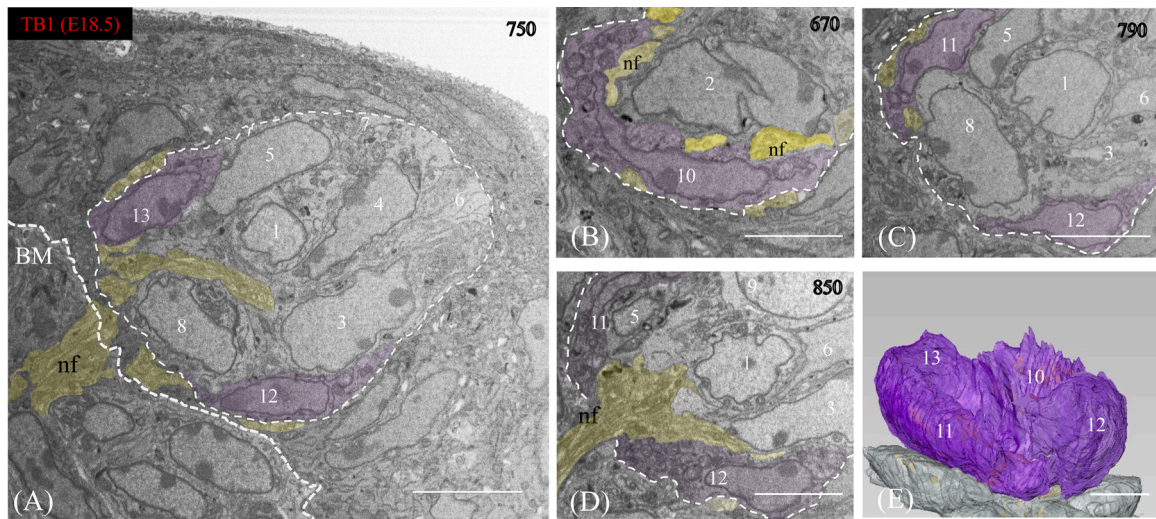


**Fig. 6.** Serial cross-sections of FIB-SEM tomography at E18.5. Basal cell arrangement. **A.** Slice number 750. Basal cells (No. 12 and 13) are thin and are in contact with the basement membrane (BM). These cells have a higher electron density than the other immature cells. The bundle of nerve fibers enters the taste bud between No. 8 and 13. These bundles comprise many thin nerve fibers, which we traced as a whole. The white dotted lines represent the taste bud boundaries. The thick white dotted line represents the BM; Scale bar: 10  $\mu\text{m}$ . **B–D.** Sections containing each basal cell (No. 10–12). The basal cells are morphologically similar to the surrounding epithelial cells and have spheroidal or disk-shaped nuclei. They lie at the bottom of the taste bud and do not protrude into the epithelial side. Basal cells and nerve fibers frequently contact each other. In slice number 850, nerve fibers enter the taste bud from the basal side. This nerve fiber is a different bundle than the nerve fiber in slice number 750. The white dotted lines represent the taste bud boundaries. nf, nerve fiber; Scale bar: 10  $\mu\text{m}$ . **E.** 3D reconstructed images of basal cells. The basal cells lie at the bottom of the taste bud (No. 10–13). Scale bar: 10  $\mu\text{m}$ .

(Fig. 9B–E, yellow). This cell had sheet-like cytoplasmic processes, which were frequently observed to embrace the nerve fibers (Fig. 9B–D). The 3D reconstructed image showed that many nerve fibers were in contact with this cell (Fig. 9F). A large number of vesicles were present

from the top of the nucleus to the tip of the cell (Fig. 9E, arrowhead).

**3.2.3.3. Type II-like cell.** There was a large cell with low cytoplasmic electron density in the middle of the P1.5 taste bud. We classified this

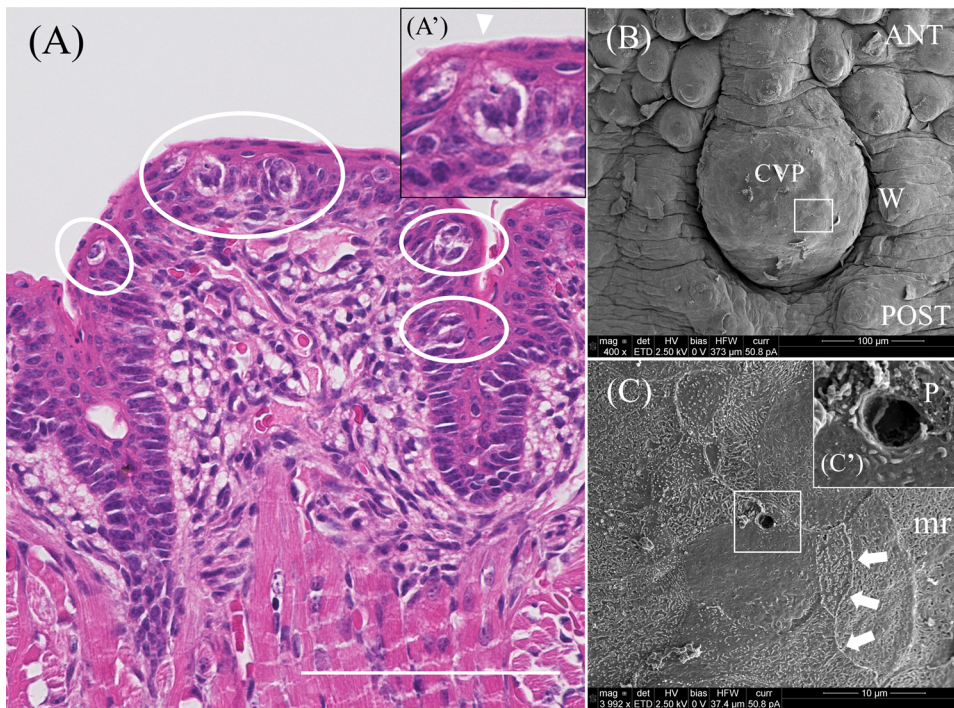


**Fig. 7.** H&E-stained section of CVP at P1.5. **A.** CVP is similar to a typical mature morphology. The trench of the CVP is still shallow. There are some immature taste buds at the top and trench of the epithelium. The size of the immature taste buds is approximately 20  $\mu\text{m}$ . Scale bar is 100  $\mu\text{m}$ . **A'.** Enlargement of the taste bud. The formation of the taste pores is not clear. **B.** SEM image of the CVP at P1.5. The CVP is slightly raised anteriorly and circularly posteriorly; the size of the CVP is approximately 300  $\mu\text{m}$  anterior (ANT) to posterior (POST) and approximately 160  $\mu\text{m}$  lateral. The CVP is surrounded by an outer lateral wall (W), and the trench within it is still shallow. **C.** Magnified image of the area enclosed by a square in B. The cell border is identified as a single raised line (white arrow), and fine micro ridges (mr) are observed on the cell surface. The epithelium has a pore with a diameter of approximately 1  $\mu\text{m}$ , but it is not clear whether it is a taste pore (square). **C'.** Magnified image of the area enclosed by a square in C. The inside of the pores is dark. The interior of the pore (P) cannot be observed darkly, and no adult-like microvilli structures were observed.

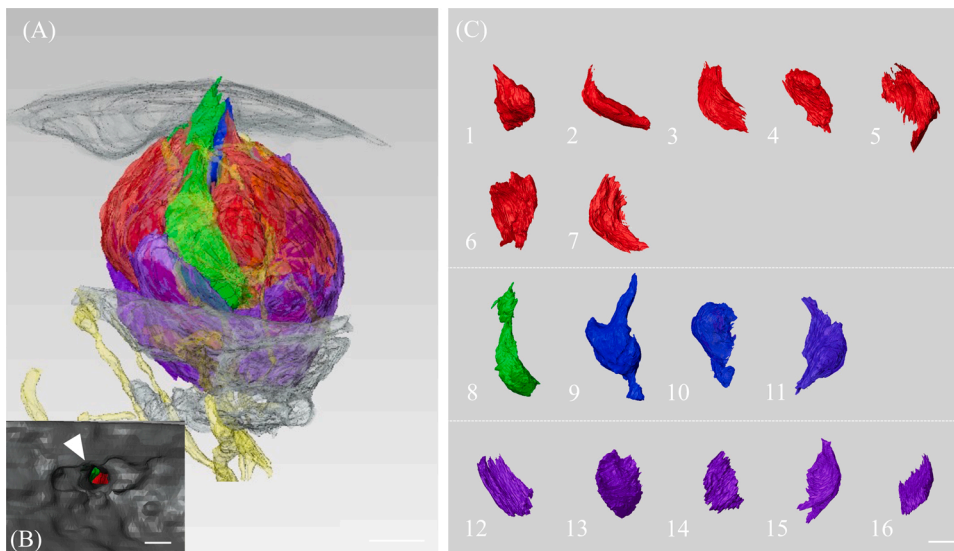


**Fig. 8.** 3D reconstructed image of the entire P1.5 CVP taste bud and each cell. **A.** The taste bud in the epithelium is onion-shaped. Nerve fibers (yellow) enter and run from the connective tissue into the taste bud. Scale bar: 10  $\mu\text{m}$ . **B.** View of the taste pores from the side of the oral cavity. Taste cells are seen in the taste pores (arrowhead). Scale bar: 2  $\mu\text{m}$ . **C.** The red cells in the upper row are classified as polymorphic cells. Most cells are directional, and some produce small processes toward the surface. The green cells (No. 8) are classified as Type I-like cells. Blue cells are Type II-like cells with glycogen in their cytoplasm, and No. 9 cell has an apical process toward the taste pore. Purple cells are Type IV cells. Type IV cells lie at the bottom of the taste bud. Scale bar: 10  $\mu\text{m}$ .

cell as a Type II-like cell (Fig. 10A, No. 9). The nucleus of this cell was round (Fig. 10A). Heterochromatin attached to the nuclear membrane was also observed. The prominent characteristic feature was the presence of many dense granules in the cytoplasm, some of which were large enough to cover the nucleus (Fig. 10A). Cells with granules in the cytoplasm were also identified in the other P1.5 taste buds (TB2) (Fig. 12A, blue cell). In addition, multiple Type II-like cells were observed in taste buds (Fig. 10A and E, No. 9–11). One of these cells (No. 9) extended its tip near the taste pore (Fig. 10B, C), and two (No. 9 and 10) had contact with the basement membrane.

**3.2.3.4. Type IV cell.** Some cells located in the basal region were classified as Type IV cells (Fig. 8C, No. 12–16). These cells were flattened and in contact with the basement membrane (Fig. 11A and B, No. 12–16). These cells had a higher electron density than the others. Type

IV cells had an irregular nucleus, and the nuclei were located at the height of 1/4 of the taste bud. The cytoplasm was thin. Substantial contact with nerve fibers entering through the basement membrane was observed; however, there was no thickening of the membrane or deformation of the nucleus at the contact area (Fig. 11B, No. 14). Most Type IV cells were flat, except for one with an irregular shape (Fig. 11B–D, No. 15). This Type IV cell extended toward the epithelium enveloping the Type II-like cell (Fig. 11C, No. 11) from the outside. In addition, the nucleus was distorted.

**3.2.3.5. Polymorphic cell.** The cells that exhibited various morphologies were classified as polymorphic cells (Fig. 8C, No. 1–7). The electron density of the cells was intermediate between the Type I-like cells and Type II-like cells (Fig. 11A, red). These cells had different nuclear shapes, either with deep invaginations (Fig. 11A, No. 2) or small

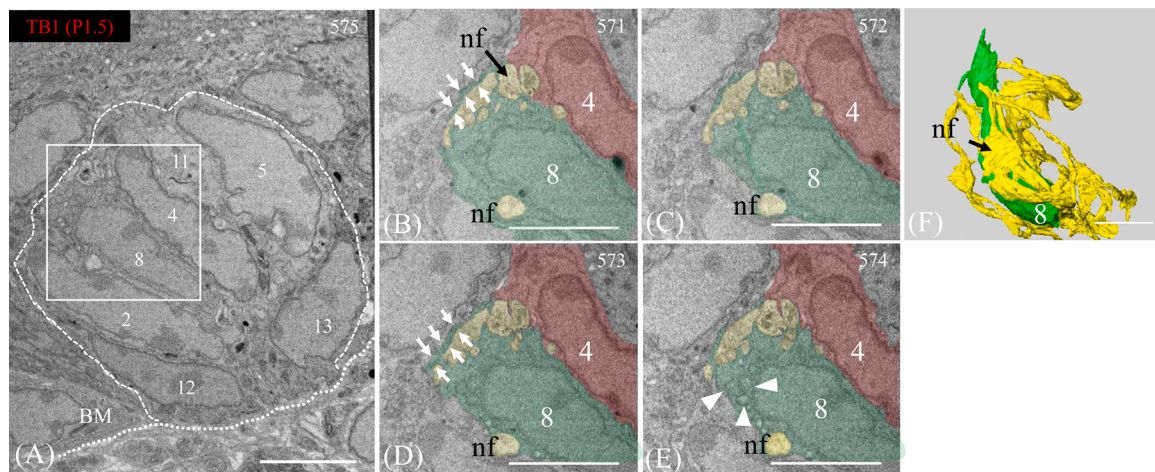


**Fig. 9.** Serial cross-sections of FIB-SEM tomography at P1.5. Characteristics of Type I-like cell at P1.5. **A.** Slice number 575. This section contains Type I-like cells and polymorphic cells. Type I-like cells have a cytoplasm with a slightly higher electron density than the surrounding polymorphic cells. The nucleus of the Type I cell (No. 8) is oval and elongate. The thin white dotted line represents the boundary of the taste bud. The thick white dotted line represents the basement membrane (BM); Scale bar: 10  $\mu\text{m}$ . **B-E.** Magnified view of the serial cross-section (No. 571–574). Type I-like cells are surrounded by polymorphic cells, and many nerve fibers run around the cell (nf; yellow). The Type I-like cell extends a thin lamella in these sections to enclose the nerve fibers (white arrow). In the cytoplasm of this cell, there are many vesicles of approximately 0.2–0.5  $\mu\text{m}$  in size (arrowheads). Scale bar: 5  $\mu\text{m}$ . **F.** 3D reconstructed image of Type I-like cell. Many nerve fibers (nf) contact Type I cells. Scale bar: 10  $\mu\text{m}$ .

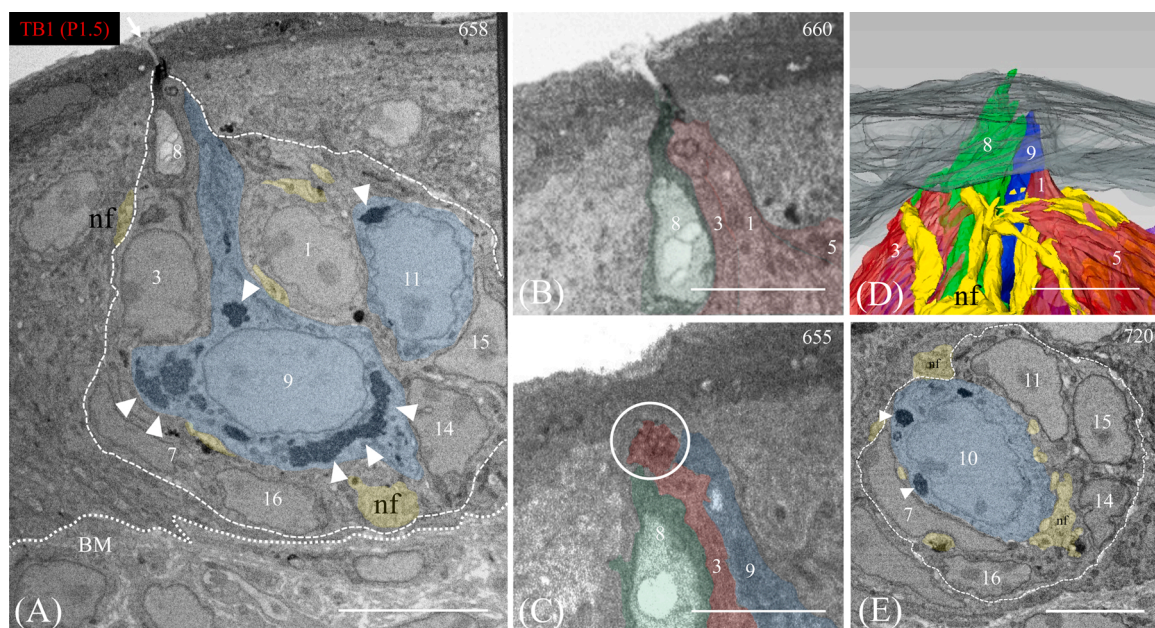


**Fig. 10.** Taste bud and their apical structure at P1.5. **A.** The taste bud is onion-shaped with a clear boundary to the surrounding epithelial cells. Type II-like cells have a lower electron density than other cells and are characterized by a round nucleus. A large Type II-like cell is present in the center of the taste bud, and aggregates of fine granules are found in their cell bodies (arrowheads). The granules surround the nucleus and are present in multiple clumps. The thin white dotted line represents the boundary of the taste bud. The thick white dotted line represents the basement membrane (BM); taste pores (arrow). nf, nerve fibers (yellow); Scale bar: 10  $\mu\text{m}$ . **B, C.** Sections around taste pores. Various cells extend through the epithelial cells toward the taste pores. Only Type I-like cells (No. 8) extend the incomplete microvilli into the small taste pores. The apical process of the other cells does not extend into the taste pores. The apical process of the No.3 cell extends under the epithelium of taste pores and finely branched (white circles). nf, nerve fibers; Scale bar: 5  $\mu\text{m}$ . **D.** 3D reconstructed image of cells around the taste pore. Light gray indicates the surrounding epithelium. The cells elongate toward the taste pores, but most of them do not yet have obvious microvilli. nf, nerve fibers run between and around cells; Scale bar: 5  $\mu\text{m}$ . **E.** Slice number 720. Type II-like cell (No. 10) also has granules in the cell body (arrow head). nf, nerve fibers (yellow); Scale bar: 10  $\mu\text{m}$ .

depressions (Fig. 11C, No. 1). The nucleus is closely associated with other cells or nerve fibers and featured invaginations of the nuclear membrane (Fig. 11A, No. 4 and 6). The major difference between the polymorphic and E18.5 immature cells was that the former had directions toward the epithelial surface layer. Most of the cells underwent a slight process in the direction of the taste pores (Fig. 10B). One polymorphic cell had an apical process just below the taste pore (No. 3,

Fig. 10B). However, the apical process did not extend into the taste pore, and the apical process branched out transversely just below the epithelium (Fig. 10C).

#### 4. Discussion

This study elucidated the structure of developing taste buds and their

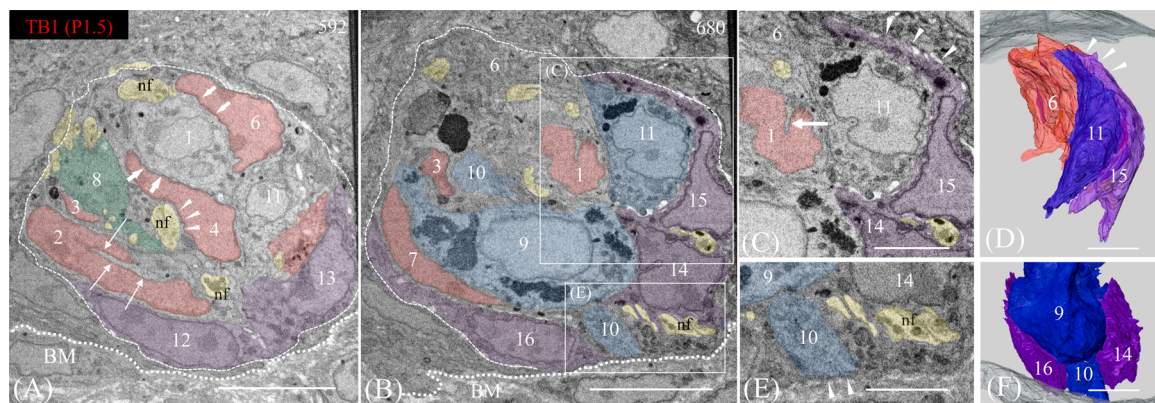


**Fig. 11.** Serial cross-sections of FIB-SEM tomography at P1.5. Type IV cells and polymorphic cells. **A.** Slice number 592. Polymorphic cells exhibit various morphologies. Some nuclei are in close proximity with other cells (thick arrows) or nerve fibers (arrowheads) and feature invaginations of the nuclear membrane. The cytoplasm in the invaginated areas is very thin. Some cell nuclei show invagination of the nuclear membrane (thin arrow). Nerve fibers (nf; yellow). The thin white dotted line represents the boundary of the taste bud. The thick white dotted line represents the basement membrane (BM). Scale bar: 10  $\mu$ m. **B.** Slice number 680. Type IV cells (No. 141516) have a nucleus in the lower 1/3 of the taste bud and high electron density. These cells are found at the base of the taste bud, and the shape of the nucleus varies. Most are oval but slightly distorted to match the surrounding cells. They are often in contact with nerve fibers (nf) entering through the basement membrane, but there is no thickening of the membrane or deformation of the nucleus at the contact site. The thin white dotted line represents the boundaries of the taste bud. The thick white dotted line represents the basement membrane (BM). Scale bar: 10  $\mu$ m. **C.** Magnified image of the area enclosed by a square in B. Unlike other Type IV cells, this Type IV cell extends its processes upward to envelop the cell (No. 11) from the outside (arrowhead). The nucleus of the polymorphic cell (No. 1) has a small invagination of the nuclear membrane (thin arrow). Scale bar: 5  $\mu$ m. **D.** 3D reconstructed images of No.6, 11, and 15. The tip of No.15 extends toward the epithelium to envelop other cells from the outside (arrowhead). Scale bar: 10  $\mu$ m. **E.** Magnified image of the area enclosed by a square in B. Type II-like cell contacts the basement membrane (arrowhead). Scale bar: 5  $\mu$ m. **F.** 3D reconstruction of the basal area shows Type II-like cells (No. 10) in contact with the basement membrane between the basal cells. Scale bar: 10  $\mu$ m.

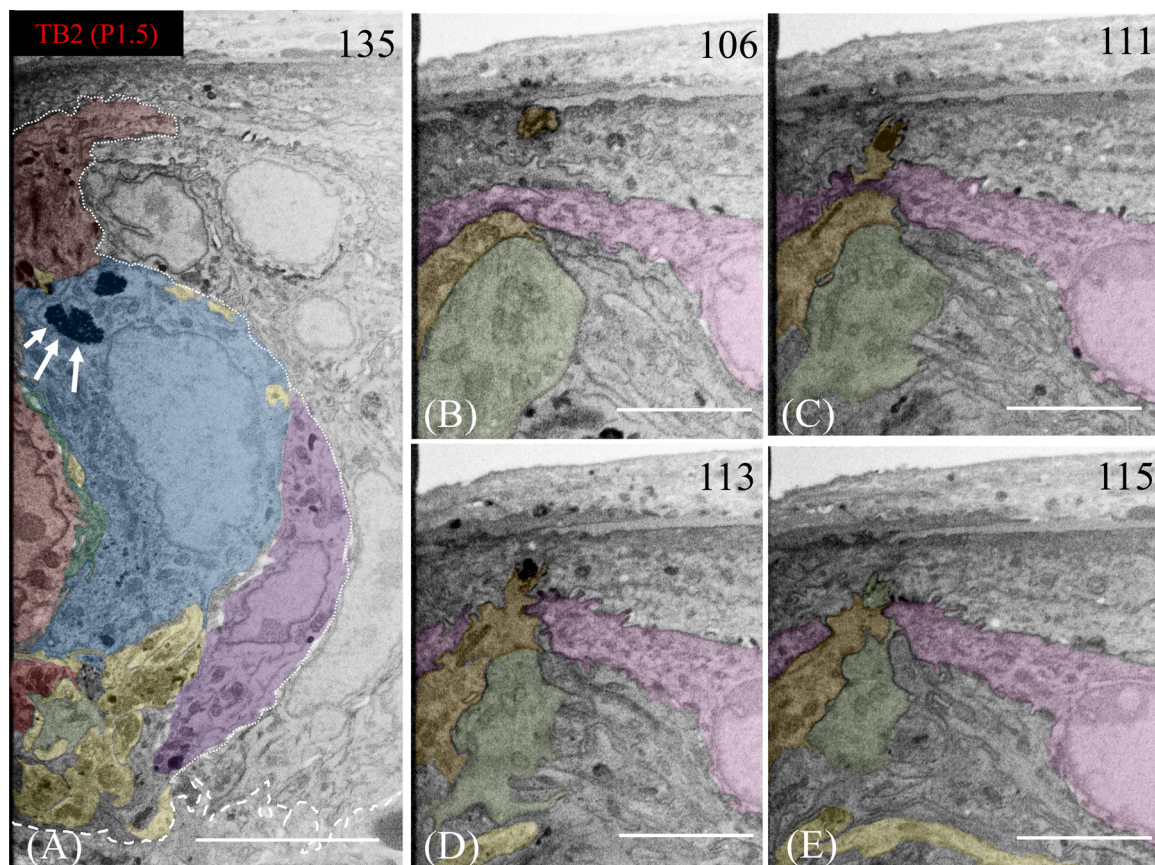


**Fig. 12.** Serial cross-sections of FIB-SEM tomography at P1.5. Taste bud of another sample of P1.5. **A.** Slice number 135. This taste bud also contains Type II-like cells (blue), which have an aggregate of fine granules in the cytoplasm (arrows). The basal part contains a large number of nerve fibers that run between the cells (yellow). The cells at the apex of the taste bud extend close to the top of the epithelium (light red). It is unclear whether a taste pore is formed because the entire taste bud is not in the image area. The thin white dotted line represents the boundary of the taste bud. The thick white dotted line represents the basement membrane. Scale bar: 10  $\mu$ m. **B-D:** Serial cross-section (No. 106 to 115). Two cells (light brown and light green) pass between the epithelial cells (light purple) and extend toward the top of the epithelium. The cell extends toward the top of the epithelium with fine processes, but it does not reach the oral cavity. Scale bar: 5  $\mu$ m.

3D ultrastructure in the CVP before and after birth in mice (Table 1). The E18.5 immature cells observed were not oriented to the epithelial surface layer (Fig. 3A). Immature cells had depressed cytoplasm and nuclei, and exhibited a variety of morphologies (Fig. 3B). These cells also did not have the specific ultrastructure of mature taste cells such as atypical mitochondria (Yang et al., 2020). In accordance with a previous study (Thirumangalathu et al., 2009), these immature cells in the embryonic stage were considered to be taste precursor cells which are poised to differentiate.

The cell extending toward the epithelial surface layer from the taste bud was observed at E18.5 (Fig. 3A). The cell body was located just below the apical surface of the epithelium, although there was no gustatory stimulation (Fig. 5B–E). Many round structures with low electron densities were observed at the extending cell body of this cell (Fig. 5). These findings are consistent with those of a previous study that identified Type II cells containing numerous vacuoles and mitochondria in the apical portion of the cells in mouse taste buds (Paran et al., 1975). Moreover, these cells are characteristic of metabolically active cells among taste cells (Farbman, 1965). Therefore, we concluded this extended cell to be a Type II like cell which may differentiate into Type II cells in the future. Early Type I and Type II cells differentiate from precursor cells (Thirumangalathu et al., 2009). Early Type II cells are thought to be actively involved in the formation and maintenance of the taste pore (Farbman, 1965). The relationship between taste pore formation and the extension of type II-like cells could not be clarified in this study. It is possible that the extension of type II-like cells is necessary before the formation of the taste pore.

The taste buds at P1.5 which appeared to have an onion-shaped morphology formed taste pores (Fig. 8A). As shown in Fig. 10B and D, cells below the taste pore formed apical processes, indicating that there might be multiple cells extending towards the taste pore. It has been shown that mature taste buds with taste pores appear at 4 days of age (Toprak and Yilmaz, 2016). Here, using FIB-SEM, we show that the taste pores are already formed at P1.5. However, the taste pores were still small, and there were no electron-dense mucous material and vesicles as seen in the taste buds of an adult. The mucous material in the taste pores, which is thought to be produced by type I cells, plays an important role in the taste perception of adult mammals (Ohmura et al., 1989; Witt and Reutter, 1996). The present results indicate that the taste cell at P1.5 has not yet begun to secrete the mucous material. Morphologically, the apical processes of the taste cells have not yet formed a complete microvillus, and therefore the taste cells of P1.5 are most likely

functionally immature. Although the formation of taste pore has been regarded as a sign of taste bud maturation (Zhang et al., 2008), we inferred that the formation of taste pore begins even when taste cells are not yet mature, and that the maturation of taste cells progresses even after the opening of taste pore. Although specific markers for type I-III cells are expressed in the embryonic stage before the formation of the taste pore (Golden et al., 2021), it is not yet clear the reason why differentiation is initiated before taste perception. The taste buds of the soft palate precede those of other papillae in the formation of the taste pore (Rashwan et al., 2016; Zhang et al., 2008). It was suggested that the spatial distribution of taste buds in the palate is important for suckling behavior immediately after birth (Harada et al., 2000). It is possible that the early taste cells are being prepared from the embryonic stage to sense nutrition soon after birth. In addition, taste cells that differentiate from taste precursor cells at an early stage may have the function of not only receiving taste, but also constructing structures unique to taste buds (e.g., formation of taste pore, cell adhesion and movement to form onion-shaped structures). Further research might be needed which will lead to morphological studies and functional analysis.

This study classified Type II-like cells of the P1.5 taste bud based on nuclear morphology, cytoplasmic electron density, and organelle morphology (Fig. 10A). Immediately after birth, the specific markers ( $\alpha$ -gustducin, PLC $\beta$ 2) for Type II cells are expressed in taste buds (Golden et al., 2021; Miura et al., 2005). The current study does not contradict this observation. Furthermore, multiple granular structures were observed in the cytoplasm of Type II-like cells (Fig. 10A) which might be glycogen because of their shape and density. Similar dense cytoplasmic granules (0.1–0.3  $\mu$ m in diameter) have been reported in fungiform papillae of E17–19 rats (Farbman, 1965) and have been considered to be a transient structure found in immature taste cells; however, their precise function is unknown. Furthermore, from the present results, we could not determine whether the predicted Type II-like cells at E18.5 and P1.5 are the same cells or not. The P1.5 taste buds contain cells that are not classified as typical Type I-III cells, and we have conveniently classified them as polymorphic cells (Fig. 8C). However, some polymorphic cells have a nuclear characteristic similar to Type III cells, suggesting they may differentiate into Type III cells in the future. The limitation of this study is that the synaptic structure between the nerve fibers, which is a characteristic of type III cells, could not be observed. Of course, the present results of this study cannot explain to which particular cell type these polymorphic cells will differentiate in the future. To explore this, the taste buds from E18.5 to P1.5 should be observed continuously using 4-dimensional analyses such as organ culture.

In the present study, drastic change of the taste bud between E18.5 and P1.5 was revealed in 3D suggesting that this period is critical for pore formation and correct arrangement of taste cells in taste buds (Figs. 3A, 8A). Recently, LGR5+ stem cells have been identified as taste stem cells, and the formation of taste bud organoids is possible from a single cell (Yee et al., 2013; Ren et al., 2014). In contrast, taste cells in taste bud organoids encounter problems to form the taste pores due to the lack of cell orientation (Aihara et al., 2015; Ren et al., 2014); therefore, further research is required to understand the mechanism of taste pore formation. In our observation, the orientation of immature taste cells was random at E18.5. When the taste pore was formed (at least by P1.5), most of the taste cells had already extended their cell process in the same direction, toward the taste pore. It is difficult to examine the signals that determine the orientation of taste cells from the present histological study. It is possible that the immature cell which extended to the surface of epithelium seen in E18.5 may differentiate and reach the epithelial surface prior to other cells and these cells follow them in the same direction. The extracellular signal-related kinases (ERKs) are closely related to cell proliferation and differentiation, and their activation in a trigger cell is transmitted to other cells and determines the direction of migration of cell populations (Aoki et al., 2017). Therefore, investigating the relationship between factors

**Table 1**  
Summary of electron microscopic features of taste cells in E18.5 and P1.5.

	E18.5	P1.5
Cell type	<ul style="list-style-type: none"> <li>• Immature taste cell (Including an extending cell in Fig. 4)</li> <li>• Basal cell</li> </ul>	<ul style="list-style-type: none"> <li>• Polymorphic cell</li> <li>• Type I-like cell</li> <li>• Type II-like cell</li> <li>• Type IV cell</li> </ul>
Shape	Spherical	Onion-shaped
Taste pore	No observed	Some taste buds have taste pore (Some taste cell has unfinished microvilli)
Electron density	<ul style="list-style-type: none"> <li>• Immature taste cell: middle (Extending cell in Fig. 4: low)</li> <li>• Basal cell: high</li> </ul>	<ul style="list-style-type: none"> <li>• Polymorphic cell: middle</li> <li>• Type I-like cell: high</li> <li>• Type II-like cell: low</li> <li>• Type IV cell: high</li> </ul>
Nucleus	<ul style="list-style-type: none"> <li>• Immature taste cell: a various shape</li> <li>• Basal cell: flat and oval</li> </ul>	<ul style="list-style-type: none"> <li>• Polymorphic cell: Irregularly indented oval nucleus</li> <li>• Type I-like cell: oval and elongated</li> <li>• Type II-like cell: round</li> <li>• Type IV cell: flat and oval</li> </ul>
Nerve	<ul style="list-style-type: none"> <li>• Contact with all cells (Some specific immature cells)</li> </ul>	<ul style="list-style-type: none"> <li>• Contact with all cells (Some specific Type I-like cell)</li> <li>• Nerve fiber branching is finer than in E18.5</li> </ul>

involved in cell migration, such as ERKs activity of taste cells and the orientation of taste cells at the stage from E18.5 to P1.5 might clarify the basic concept of morphogenesis. We speculate that this could provide insights for culture and regeneration studies.

At E18.5 and P1.5, taste buds were detected in the apical epithelium facing the oral cavity (Figs. 2 and 7) and our FIB-SEM images also captured the taste buds from the apical epithelium of the CVP. There are two perspectives on the development of primitive taste buds. One is that the taste buds of the CVP differentiate in the dorsal epithelium of the CVP at P0 (Uchida et al., 2003), and the other is that they first differentiate in the trench epithelia during the first postnatal week (Krimm et al., 2015). Taste placodes express Shh (Hall et al., 1999; Jung et al., 1999), which are defined as taste bud precursor cells (Thirumangalathu et al., 2009). Shh is expressed in the epithelial apex of the CVP at E12.5 when taste placodes are formed (Zhang et al., 2020). Therefore, taste placodes are thought to be formed from the epithelial apex of the CVP. Taken together, the findings of this study support the theory that immature taste buds are formed from the epithelium at the top of the papillae. Immediately after birth, when the trench of the CVP has not been fully formed, only the top of the papillae can receive taste stimuli. Therefore, it is likely that taste bud formation begins at the top of the papillae to receive taste stimuli early.

## 5. Conclusion

In this study, we unraveled the morphological details of the taste bud cells at E18.5 and P1.5 (Table 1). The taste bud at E18.5, when gustatory stimulation has not yet started, did not have a taste pore and was spherical. One of the immature cells was observed to extend a process from taste bud but it did not reach the apical surface or the oral cavity. The taste bud at P1.5, when gustatory stimulation has started, had a taste pore and an onion-shaped arrangement like a matured taste bud, and was most likely able to perceive taste. The cells extended to the taste pore but did not exhibit the morphology of adult taste cells yet. Our findings also demonstrated that taste pores are formed before the taste buds mature. In addition, this study revealed that there were no obvious mature taste cells at either time point and the maturation of taste cells progresses after the opening of taste pore. Further detail classification of the immature cells in early taste buds using immuno-electron microscopy and/or quantitative analysis would make the timeline of taste bud differentiation clearer.

## Author contributions

**Kiyosato Hino:** Conceptualization Writing- original draft, Software, Investigation, Visualization, Formal analysis **Shingo Hirashima:** Writing-Reviewing and Editing **Risa Tsuneyoshi:** Resources **Akinobu Togo:** Data curation, Resources **Tasuku Hiroshige:** Supervision **Jingo Kusukawa:** Project Administration **Kei-Ichiro Nakamura:** Project Administration **Keisuke Ohta:** Resources, Methodology

## Funding source

This research did not receive any specific grant from funding agencies in the public, commercial, or not-for-profit sectors.

## Declaration of Competing Interest

The author(s) declare no potential conflicts of interest with respect to the research, authorship, and/or publication of this article.

## Acknowledgments

We thank Mr. Kei-Ichiro Uemura for his technical assistance with the experiments. We also thank Editage ([www.editage.com](http://www.editage.com)) for English language editing.

## Appendix A. Supplementary data

Supplementary material related to this article can be found, in the online version, at doi:<https://doi.org/10.1016/j.tice.2021.101714>.

## References

- Aihara, E., Mahe, M.M., Schumacher, M.A., Matthis, A.L., Feng, R., Ren, W., Noah, T.K., Matsu-Ura, T., Moore, S.R., Hong, C.I., Zavros, Y., Herness, S., Shroyer, N.F., Iwatsuki, K., Jiang, P., Helmuth, M.A., Montrose, M.H., 2015. Characterization of stem/progenitor cell cycle using murine circumvallate papilla taste bud organoid. *Sci. Rep.* 5, 1–15. <https://doi.org/10.1038/srep17185>.
- Aoki, K., Kondo, Y., Naoki, H., Hiratsuka, T., Itoh, R.E., Matsuda, M., 2017. Propagating wave of ERK activation orients collective cell migration. *Dev. Cell* 43. <https://doi.org/10.1016/j.devcel.2017.10.016>, 305–317.e5.
- Barlow, L.A., 2015. Progress and renewal in gustation: new insights into taste bud development. *Development* 142, 3620–3629. <https://doi.org/10.1242/dev.120394>.
- Chaudhari, N., Roper, S.D., 2010. The cell biology of taste. *J. Cell Biol.* <https://doi.org/10.1083/jcb.201003144>.
- Denk, W., Horstmann, H., 2004. Serial block-face scanning electron microscopy to reconstruct three-dimensional tissue nanostructure. *PLoS Biol.* 2 <https://doi.org/10.1371/journal.pbio.0020329>.
- Farbman, A.I., 1965. Electron microscope study of the developing taste bud in rat fungiform papilla. *Dev. Biol.* 11, 110–135. [https://doi.org/10.1016/0012-1606\(65\)90040-0](https://doi.org/10.1016/0012-1606(65)90040-0).
- Golden, E.J., Larson, E.D., Shechtman, L.A., Trahan, G.D., Gaillard, D., Fellin, T.J., Scott, J.K., Jones, K.L., Barlow, L.A., 2021. Onset of taste bud cell renewal starts at birth and coincides with a shift in shh function. *Elife* 10, 1–28. <https://doi.org/10.7554/eLife.64013>.
- Hall, J.M., Hooper, J.E., Finger, T.E., 1999. Expression of Sonic hedgehog, patched, and Gli1 in developing taste papillae of the mouse. *J. Comp. Neurol.* 406, 143–155. [https://doi.org/10.1002/\(SICI\)1096-9861\(19990405\)406:2<143::AID-CNE1>3.0.CO;2-X](https://doi.org/10.1002/(SICI)1096-9861(19990405)406:2<143::AID-CNE1>3.0.CO;2-X).
- Harada, S., Yamaguchi, K., Kanemaru, N., Kasahara, Y., 2000. Maturation of taste buds on the soft palate of the postnatal rat. *Physiol. Behav.* 68, 333–339. [https://doi.org/10.1016/S0031-9384\(99\)00184-5](https://doi.org/10.1016/S0031-9384(99)00184-5).
- Hirashima, S., Ohta, K., Kanazawa, T., Okayama, S., Togo, A., Uchimura, N., Kusukawa, J., Nakamura, K.I., 2016. Three-dimensional ultrastructural analysis of cells in the periodontal ligament using focused ion beam/scanning electron microscope tomography. *Sci. Rep.* 6, 1–9. <https://doi.org/10.1038/srep39435>.
- Jung, H.S., Oropeza, V., Thesleff, I., 1999. Shh, Bmp-2, Bmp-4 and Fgf-8 are associated with initiation and patterning of mouse tongue papillae. *Mech. Dev.* 81, 179–182. [https://doi.org/10.1016/S0925-4773\(98\)00234-2](https://doi.org/10.1016/S0925-4773(98)00234-2).
- Kapsimali, M., Barlow, L.A., 2013. Developing a sense of taste. *Semin. Cell Dev. Biol.* 24, 200–209. <https://doi.org/10.1016/j.semcdb.2012.11.002>.
- Kato, M., Ito, T., Aoyama, Y., Sawa, K., Kaneko, T., Kawase, N., Jinnai, H., 2007. Three-dimensional structural analysis of a block copolymer by ScanningElectron microscopy combined with a focused ion beam. *J. Polym. Sci.* 45, 677–683. <https://doi.org/10.1002/polb.21088>.
- Kim, Jae Young, Lee, M.J., Cho, K.W., Lee, J.M., Kim, Y.J., Kim, Ji Youn, Jung, H.I., Cho, J.Y., Cho, S.W., Jung, H.S., 2009. Shh and ROCK1 modulate the dynamic epithelial morphogenesis in circumvallate papilla development. *Dev. Biol.* 325, 273–280. <https://doi.org/10.1016/j.ydbio.2008.10.034>.
- Kinnamon, J.C., Yang, R., 2008. Ultrastructure of Taste buds. In: Basbaum, A., Kaneko, A., Shepherd, G., Westheimer, G. (Eds.), *The Senses: A Comprehensive Reference*. UK, pp. 135–155.
- Knott, G., Marchman, H., Wall, D., Lich, B., 2008. Serial section scanning electron microscopy of adult brain tissue using focused ion beam milling. *J. Neurosci.* 28, 2959–2964. <https://doi.org/10.1523/JNEUROSCI.3189-07.2008>.
- Kramer, N., Chen, G., Ishan, M., Cui, X., Liu, H.X., 2019. Early taste buds are from Shh+ epithelial cells of tongue primordium in distinction from mature taste bud cells which arise from surrounding tissue compartments. *Biochem. Biophys. Res. Commun.* 515, 149–155. <https://doi.org/10.1016/j.bbrc.2019.05.132>.
- Kremer, A., Lippens, S., Bartunkova, S., Asselbergh, B., Blanpain, C., Fendrych, M., Goossens, A., Holt, M., Janssens, S., Krols, M., Larsimont, J.C., Mc Guire, C., Nowack, M.K., Saelens, X., Schertel, A., Schepens, B., Slezak, M., Timmerman, V., Theunis, C., Van Brempt, R., Visser, Y., Guérin, C.J., 2015. Developing 3D SEM in a broad biological context. *J. Microsc.* 259, 80–96. <https://doi.org/10.1111/jmi.12211>.
- Krimm, R.F., Thirumangalathu, S., Barlow, L.A., 2015. Development of the Taste system. In: Doty, Richard L. (Ed.), *Handbook of Olfaction and Gustation, third edition*, pp. 727–747.
- Liman, E.R., Zhang, Y.V., Montell, C., 2014. Peripheral coding of taste. *Neuron* 81, 984–1000. <https://doi.org/10.1016/j.neuron.2014.02.022>.
- Micheva, K.D., Smith, S.J., 2007. Array tomography: a new tool for imaging the molecular architecture and ultrastructure of neural circuits. *Neuron* 55, 25–36. <https://doi.org/10.1016/j.neuron.2007.06.014>.
- Mistretta, Charlotte M., Liu, H.-X., 2006. Development of fungiform papillae: patterned lingual gustatory organs. *JSTAGE*. <https://doi.org/10.1679/aohc.69.199>.
- Miura, H., Kato, H., Kusakabe, Y., Ninomiya, Y., Hino, A., 2005. Temporal changes in NCAM immunoreactivity during taste cell differentiation and cell lineage relationships in taste buds. *Chem. Senses* 30, 367–375. <https://doi.org/10.1093/chemse/bji031>.

- Miura, H., Kusakabe, Y., Hashido, K., Hino, A., Ooki, M., Harada, S., 2014. The glossopharyngeal nerve controls epithelial expression of Sprr2a and Krt13 around taste buds in the circumvallate papilla. *Neurosci. Lett.* 580, 147–152. <https://doi.org/10.1016/j.neulet.2014.08.012>.
- Nakayama, A., Miura, H., Shindo, Y., Kusakabe, Y., Tomonari, H., Harada, S., 2008. Expression of the basal cell markers of taste buds in the anterior tongue and soft palate of the mouse embryo. *J. Comp. Neurol.* 509, 211–224. <https://doi.org/10.1002/cne.21738>.
- Ogata, T., Ohtubo, Y., 2020. Quantitative analysis of taste bud cell numbers in the circumvallate and foliate taste buds of mice. *Chem. Senses* 45, 261–273. <https://doi.org/10.1093/chemse/bjaa017>.
- Ohmura, S., Horimoto, S., Fujita, K., 1989. Lectin cytochemistry of the dark granules in the type 1 cells of Syrian hamster circumvallate taste buds. *Arch. Oral Biol.* 34, 161–166. [https://doi.org/10.1016/0003-9969\(89\)90003-4](https://doi.org/10.1016/0003-9969(89)90003-4).
- Ohta, K., Sadayama, S., Togo, A., Higashi, R., Tanoue, R., Nakamura, Kichiro, 2012. Beam deceleration for block-face scanning electron microscopy of embedded biological tissue. *Micron* 43, 612–620. <https://doi.org/10.1016/j.micron.2011.11.001>.
- Paran, N., Mattern, C.F.T., Henkin, R.I., 1975. Ultrastructure of the taste bud of the human fungiform papilla. *Cell Tissue Res.* 161, 1–10. <https://doi.org/10.1007/BF00222109>.
- Rashwan, A., Konishi, H., El-Sharaby, A., Kiyama, H., 2016. Ontogeny and innervation of taste buds in mouse palatal gustatory epithelium. *J. Chem. Neuroanat.* 71, 26–40. <https://doi.org/10.1016/j.jchemneu.2015.11.003>.
- Ren, W., Lewandowski, B.C., Watson, J., Aihara, E., Iwatsuki, K., Bachmanov, A.A., Margolskee, R.F., Jiang, P., 2014. Single Lgr5- or Lgr6-expressing taste stem/progenitor cells generate taste bud cells ex vivo. *Proc. Natl. Acad. Sci. U. S. A.* 111, 16401–16406. <https://doi.org/10.1073/pnas.1409064111>.
- Royer, S.M., Kinnamon, J.C., 1991. HVEM serial-section analysis of rabbit foliate taste buds: I. Type III cells and their synapses. *J. Comp. Neurol.* 306, 49–72. <https://doi.org/10.1002/cne.903060105>.
- Royer, S.M., Kinnamon, J.C., 1994. Application of serial sectioning and three-dimensional reconstruction to the study of taste bud ultrastructure and organization. *Microsc. Res. Tech.* 407, 381–407. <https://doi.org/10.1002/jemt.1070290508>.
- Seta, Y., Toyoshima, K., 1995. Three-dimensional structure of the gustatory cell in the mouse fungiform taste buds: a computer-assisted reconstruction from serial ultrathin sections. *Anat. Embryol. (Berl)*. 191, 83–88. <https://doi.org/10.1007/BF00186781>.
- Thirumangalathu, S., Barlow, L.A., 2015.  $\beta$ -Catenin signaling regulates temporally discrete phases of anterior taste bud development. *Development* 142, 4309–4317. <https://doi.org/10.1242/dev.121012>.
- Thirumangalathu, S., Harlow, D.E., Driskell, A.L., Krimm, R.F., Barlow, L.A., 2009. Fate mapping of mammalian embryonic taste bud progenitors. *Development* 136, 1519–1528. <https://doi.org/10.1242/dev.029090>.
- Toprak, B., Yilmaz, S., 2016. Light and scanning electron microscopic investigation of postnatal development of vallate papillae in the white laboratory mice. *Ataturk Univ. Vet. Bilim. Derg.* 11, 131–137. <https://doi.org/10.17094/avbd.04368>.
- Uchida, N., Kanazawa, M., Suzuki, Y., Takeda, M., 2003. Expression of BDNF and TrkB in mouse taste buds after denervation and in circumvallate papillae during development. *Arch. Histol. Cytol.* <https://doi.org/10.1679/aohc.66.17>.
- Witt, M., Reutter, K., 1996. Embryonic and early fetal development of human taste buds: a transmission electron microscopical study. *Anat. Rec.* 246, 507–523. [https://doi.org/10.1002/\(SICI\)1097-0185\(199612\)246:4<507::AID-AR10>3.0.CO;2-S](https://doi.org/10.1002/(SICI)1097-0185(199612)246:4<507::AID-AR10>3.0.CO;2-S).
- Yang, R., Dzowo, Y.K., Wilson, C.E., Russell, R.L., Kidd, G.J., Salcedo, E., Lasher, R.S., Kinnamon, J.C., Finger, T.E., 2020. Three-dimensional reconstructions of mouse circumvallate taste buds using serial blockface scanning electron microscopy: I. Cell types and the apical region of the taste bud. *J. Comp. Neurol.* 528, 756–771. <https://doi.org/10.1002/cne.24779>.
- Yee, K., Li, Y., Redding, K.M., Iwatsuki, Ken, Margolskee, R.F., Jiang, P., 2013. Lgr5-EGFP marks taste bud stem / progenitor cells in posterior tongue. *Stem Cells* 31, 992–1000. <https://doi.org/10.1002/ber>.
- Zhang, G.H., Zhang, H.Y., Deng, S.P., Qin, Y.M., Wang, T.H., 2008. Quantitative study of taste bud distribution within the oral cavity of the postnatal mouse. *Arch. Oral Biol.* 53, 583–589. <https://doi.org/10.1016/j.archoralbio.2008.01.005>.
- Zhang, S., Lee, J.M., Ashok, A.A., Jung, H.S., 2020. Action of actomyosin contraction with shh modulation drive epithelial folding in the circumvallate papilla. *Front. Physiol.* 11, 1–12. <https://doi.org/10.3389/fphys.2020.00936>.